Acta Scientific Pharmacology

Volume 3 Issue 1 January 2022

Research Article

CFD Analysis of Blood Flow and Drug Concentration Distribution in Tumor Affected Cerebral Artery-tissue Region

Sindhuja Moda[1] and Pradip Majumdar[2]*

[1]*Department of Mechanical Engineering, Northern Illinois University, USA*

[2]*DSinnovtech, Inc, USA*

***Corresponding Author:** Pradip Majumdar, DSinnovtech, Inc, USA.

Received: September 23, 2021

Published: December 30, 2021

Abstract

Brain tumors occur in the brain with the growth of abnormal cells. Despite the advancements in medical technologies and treatments, the complex geometry of the brain impedes the treatment of tumors in the brain. A promising and efficient drug targeting to the diseased regions with limited dosage input reduces the risk of potential damage of healthy- tissue cells in the vicinity of tumor. Insertion of drug particles into the bloodstream through intravenous administration is one of the efficient treatment methods which is gaining importance. Currently, extensive research is being conducted in the areas of treating brain tumors effectively with direct administration of drug through blood. In this study a three- dimensional computational simulation model of the artery capillary network with cerebral part is developed and reconstructed using multiple CT and MRI scan images of a tumor-affected patient. The simulation model includes solution of governing equations of blood flow dynamics based on Navier-Stokes equations and mass species transport based on Lagrangian particle flow dynamics in the artery network and capillaries of the adjacent tissue-tumor regions subjected to typical cardiac cycle. Computational analysis is performed to evaluate and analyze the blood flow and drug-particle distributions around the targeted region with varying concentrations. The main objective of this study is to evaluate and optimize the effectiveness of the drug delivery to the internal targeted tumor region for different input drug parameters such as drug type, density, and dose concentrations.

Keywords: Blood Flow; Brain Tumor; Lagrangian Flow

Introduction

Now a days improved medical technologies are available for efficient treatment for many dreadful diseases, including cancer. However, despite the efficient treatments, brain tumors are one of the leading causes of mortality. According to the statistical estimation of National Brain Tumor Society, the average mortality rate of adult malignant brain tumors is 3.3%. Brain tumors can originate with the growth of tumor cells within the brain or by tumor cells migrated from another part as a secondary tumor. Brain tumors come under a special category of cancers as the brain's blood-brain-barrier (BBB) resists the intake of external agents given as drugs to treat cancer in the brain. Currently, extensive research is being conducted in the areas of treating brain tumors effectively crossing the barriers of the blood brain barrier with direct administration of drug through blood. However, administration of drug is to be in safe limits of dosage. Excess dosage given to target the tumor reaching through blood-brain barrier may harm the healthy cells around the targeted area of the body. This study is on the development of a three-dimensional simulation analysis model of tumor affected brain with a blood- supplying artery integrated to it and analyzing the drug particle movements with various parameters such as dosage, particle size, and estimate of the safe level of drug administration to treat the targeted area successfully.

Brain tumors occur in the brain with the growth of abnormal cells. Despite the advancements in medical technologies and treat-

ments, the complex geometry of the brain impedes the treatment of tumors in brain. A promising and efficient drug targeting to the diseased regions with the limited dosage inputs is essential to reduce the risk of potential damage of healthy cells and tissues in the vicinity of tumor. Insertion of drug particles into the bloodstream through intravenous administration is one of the treatment methods available in treating tumor cells. In this method the tumor cells are directly targeted by the drug particles which flow with the blood. Typical dosages of drugs are administered to the patients depending on the extent of spread of tumor. Constant research is being carried out in improving the drugs targeting efficiency by changing parameters such as dosage increments and particle's dimensions depending on the severity. Padole., *et al.* [1] studied analysis of pulsatile blood flow in healthy and atherosclerosis -affected artery. The study is carried out with changes in flow field. They compared both steady and transient flow of blood and the results showed that transient flow gives accurate results of analysis to the steady-state case. This study helped me in my work in setting the velocity inlet boundary condition for accurate results and for reference in analysing the results of the blood flow for given cardiac flow with varied velocities with respect to time.

Khaled and Vafai [2] mainly explain and derives various models available for setting porous medium for biological tissues. Using mass diffusion and different convective models, transport in porous media is reviewed. Their study shows the applications of several models and suitability of flow models for various flow types. This study is useful to find the suitable flow model for the different regions of the human body. Using the list of suitability mentioned in this study, the brinkman's model is considered for this case as it is the best fit of all the models for the tissues nearer to the capillaries as explained by their study.

Yamaguchi., *et al.* [3] studied fluid flow analysis on micro-and macro-scale hemodynamic. Their study includes analysis on arteries and capillaries using numerical methods. This paper mainly discussed the advantages and disadvantages of several methods such as bending element method and volume of method. This study is helpful in analyzing the flow in minor blood flow in minute vessels like capillaries. Yilmaz and Gundogdu [4] have shown viewpoints on analysis of blood viscosity model and physiological flow conditions using experimental viscosity data. The set of experimental values of cardiac input is considered and the model is analysed for pressure and velocities of blood flow making changes to viscosity models. They have explained that Carreau-Yasuda model is appropriate for non-Newtonian flow of blood. For my work this paper is used as a basic guide to define accurate viscosity model for the given condition to avoid errors.

Arfin., *et al.* [5] in their study explained the distribution of the drug in the brain-tumor coupled to its physio-chemical properties. Their study includes design of a realistic three-dimensional tissue geometry extracted from MRI images of a brain tumor for analysis as a primary step and analyze the flow of blood in tumor considering the diffusion, reaction and convection models in which Darcy's law is used to account for the convective contribution of the interstitial fluid. This study is useful for analysing the blood flow in realistic brain using Darcy model. Bello and Carroll [6] studied and evaluated the efficiency of combined chemotherapy drugs in treating the targeted area of human gliomas. But their study was initially limited to mice. They used carboplatin and etoposide as the two chemotherapeutic drugs. Their attempted treatment caused a decrease in tumor volume, which shows an added advantage of the treatment, but with several severe side effects.

Shafiullah and Majumdar [7] in their study analysed the blood flow dynamics three-dimensional straight artery with a branched structure with and without stenosis. A cardiac cycle for pressure waveform was derived from experimental data in the simulation analysis to evaluate the stented arteries. This study was helpful in setting up the physics for the present study and used as a guide for analysing the blood flow in unsteady case. Narmada [8] in her study extended the model presented by Shafiullah and Majumdar [7] of branched straight artery to a much realistic artery network derived from the CT scan of atherosclerosis patient. She also extended the model to include a porous medium based on Darcy's flow dynamics model for blood flow through artery network including a tissue region. This work is used in this study for setting up the porous media formulation for blood transport through tissue- tumor region.

The main objective of this study is to evaluate and optimize the effectiveness of the drug delivery to the internal targeted tumor region for different input drug parameters such as drug type, density, and dose concentrations. The objective is to design the realistic three- dimensional artery network connected to a tumor-tissue of the cerebral system and to analyse the blood flow and drug concentration distribution in the artery-capillary-cerebral network. For this study, the artery-capillary network with cerebral part is mod-

eled and reconstructed using multiple CT and MRI scan images of a tumor-affected patient. The simulation model includes solution of governing equations of blood flow dynamics based on Navier-Stokes equations and mass species transport based on Lagrangian particle flow dynamics in the artery network and capillaries of the adjacent tissue-tumor regions subjected to typical cardiac cycle. A computational analysis is performed to evaluate and analyse the blood flow and drug particle distributions around the targeted region. In this study the particle administration is assumed to be done directly through intra-venal method and the administration is analysed with varying concentrations and particle diameter to identify the possibilities of treating the targeted region effectively with prescribed safe level of dosage causing no harm to healthy cells around the target. The main objective of this study is to evaluate and optimize the effectiveness of the drug delivery to the internal targeted tumor region for different input drug parameters such as drug type, density, and dose concentrations.

Blood flow in brain and brain tumors

In this section, a brief description of the human body circulatory system, characteristics of the blood flow dynamics in artery-capillary network, cerebral-network and details of brain tumor and its treatment methods are given.

Circulatory system

Human circulatory system consists of heart which acts as pump and the blood vessels which carry blood to and from the heart in respective cycles. This cardiovascular system's structure is designed to provide the body with oxygen, nutrients and to remove waste from tissue cells. Blood flows into the heart through veins and flows away from the heart through arteries. However, flow of blood to various organs is worth noticing as it involves series of changes in flow diameter from start point to the target. The oxygenated blood carried by arteries is taken from the aorta, which is the biggest direct vessel connected to heart. From arteries, blood flows into smaller vessels called arterioles, which divide into even smaller vessels called capillaries [9]. The exchange of spices and energies takes place from capillaries to the cells and deoxygenated blood merges into venules and then into larger veins.

Cardiac cycle

Cardiac cycle explains the pumping mechanism of the heart. figure 1 shows a typical such velocity artery waveform.

Figure 1: A typical artery wave form.

The blood flow waveform is described in terms of the following parameters: Systolic forward peak velocity (V_F), Diastolic reverse peak velocity (V_R), End diastolic velocity (V_D) and Time-averaged mean velocity (V_M). The femoral flow velocity increased rapidly in early systole and reached peak velocity (V_F) and it reduces gradually to the minimum reverse velocity (V_R). The deceleration time is comparatively shorter than the acceleration time. The amplitude of the reverse flow velocity is smaller than the forward flow velocity and greater than the diastolic flow velocity.

Blood vessels and flow network

Blood vessels spread all over the body, originating from the heart to supply and draw blood from different body parts. The size of the vessels varies with the amount of the blood carried by them. There are three types of blood vessels. Arteries carry oxygenated blood from heart to all the body parts. The flow of blood exerts high pressure on arteries as most of the force is exerted by the blood while leaving the heart. To withstand this high pressure, artery walls are more elastic, thicker, and muscular than all other vessel walls of the circulatory system. The high elasticity elastic tissues of arteries allow them to expand and contract and stand higher pressures. Muscular nature offers smoothness to the arteries which allows them to expand and contract it, resulting in regulating the blood flow [7,8].

Like arteries, arterioles carry blood rich in oxygen to body parts. These are the subdivisions of arteries and are narrower than the arteries. They are thinner in size as they face less pressures than the arteries. However, they are muscular in nature like the parent vessel artery and thus efficiently regulate the blood flow through a

series of expansions and contractions whenever required. Capillaries are the smallest of all the blood vessels in the body and connects to all the various organs of the entire body. They have the thinnest structure with only a thin permeable layer called endothelium, which acts as the barrier between the tissues and the blood in capillaries. The permeability of the layer allows the blood to exchange the nutrients and oxygen as energy to the tissues. Also, the waste gases are in turn taken out from the tissue and carried away by the blood through this layer in capillaries. The exhaust derived from the tissues is carried to venules from capillaries [7,8]. The figure 2 gives an idea of the blood flow.

Figure 1: Figure 2: Gives an idea of the blood flow. (Source: https://en.wikipedia.org/wiki/Capillary. http://www.medicalexhibits.com/medical_exhibits_image.php?exhibit=09079-36).

Veins and venules network

Deoxygenated blood from the capillaries is to be carried back to heart for repetition of cycle. This is done by veins in our circulatory system. Veins are thinner and less elastic in nature compared to arteries as they are offered with under less pressures throughout the cycle. The underlying mechanism in pushing the blood back to the heart depends on the inertia, gravity, and the muscle contraction force. This contraction force helps in forcing blood to the heart. Venule's function is like the arterioles, but it collects and supplies the deoxygenated blood from back to the heart instead of supplying blood from the heart as arterioles [2]. Tissues are made of series of discontinuous functional units connected. Many capillaries combine and form the tissue. The outermost layer of tissues is made of muscles which are in turn made of blood vessels, capillaries, and connective tissue [8].

Brain and blood flow

Brain structure

It is the most complex and heaviest organ of the human body responsible for the control over the action of the entire system. It weighs around three pounds and requires 746 ml of blood flow for every minute. Brain and spinal cord together constitute the central nervous system and function primarily as a unit that receives signals as inputs in the form of physical and chemical entities and interprets the information to control the body's response. Brain is also responsible for monitoring blood pressure and hormonal balances in the body. It has several parts with unique functionalities in controlling the bodily actions [10]. In this study CT scan image of basilar artery-capillary network is considered. So, the study is basically involving analysis of blood flow in the tumor regions of posterior cerebrum.

Cerebral blood flow

Coronary artery arising from the heart divides into several branches to supply the blood in neck, throat, and brain regions. The blood supply to the brain is carried by the two pair of arteries called internal-carotid and basilar artery. These arteries originate from internal carotid artery and vertebral artery which branches from the coronary artery and subclavian artery of heart. These major arteries again sub-branch into anterior, middle, and posterior cerebral arteries to supply blood to various parts of the brain. The anterior cerebral artery supplies blood to the middle and front portions of brain and posterior cerebral artery supplies blood to brain stem and back portion of brain.

Brain tumors

Growth of abnormal cells in the tissues and other parts of brain leads to brain tumor. These tumors may originate within the brain or developed due to the transfer of tumor cells from another part of the body. These developed tissues avoid flow of blood and nutrients to the essential parts of brain resulting in functional abnormalities [10]. Tumor's origin is deciding factor to categorize them as primary or secondary tumors. Primary tumors originate within the brain, whereas the secondary tumors are derivatives of body tumors that finally reach the brain. The part of the brain being affected: Tumor types are decided depending on the type or part of the organ where it arises. Brain can be affected with tumor in its tissues, brain stem and some other tiny parts within the brain. However, brain tumors which originate in the tissues are most common and are responsible for many deaths.

In this study, a tumor originated in the tissue of the brain connected to basilar artery is considered. The MRI scans considered in designing the model for analysis are shown in figure 3.

The above MRI scan image (Figure) is of a patient suffering from grade III astrocytoma. Astrocytoma arises from the cells called astrocytes which are the network of glial cells. The scans show the area of existence of tumor and its extent of spread. From the scans both sagittal and axial, it is evident that the woman has an abnormal mass spreading from left to right [11]. Also, the intensity of signals is shown predominantly in the right parietal lobe with an extension to corpus callosum.

Figure 3: MRI scan of Diseased Patient. (Source: http://emedicine.medscape.com/article/336695-overview)

Treatment methods

Several treatment methods are available for treating brain tumors. However, these methods depend on factors such as type, location, and size of the tumor [10]. The following are the treatment options available.

Steroids

These are the hormones given in fixed dosages for a fixed period to reduce the growth of tumors. Steroids cannot cure the tumor permanently, but they promote the growth inhibition. Surgery: It is the traditional treatment done as an initial attempt to remove abnormal mass from the brain. Surgery such as biopsy, partial removal or debulking is beneficial in treating tumors which are huge and hard to control. However, risks include infections, blood clots and more recovery time. Chemotherapy: This process involves delivery of anti-cancer drug, travelling through the bloodstream to reduce the tumor growth. This procedure offers promising results without the necessity of surgery with some potential risks like any other treatments. Radiation Therapy*:* This therapy involves treatment using external beam radiation to kill the cancer cells. This treatment is used to the parts of brain where surgery is not possible to perform. Unlike surgery it offers chance of avoiding seizures and infections through surgery.

Stereotactic radiosurgery

This is the new approach which is being used now-a-days. In this method radiations are targeted to the exact vicinity of the tumor thereby reducing the damage to the healthy tissues surrounding the tumor. This method also offers more flexibility and avoids surgery.

The list of anticancer drugs and its properties are shown in table 1. These drugs are most used in treating the brain tumor as they can penetrate the brain. table 1 gives the molecular formula and density of each the drug.

Anti-cancer drugs for treating tumors

In this study, treating of brain's tumor through injection of various concentrations of drug into the blood flow is observed. In this procedure several common intravenous anti-cancer drugs are used for analysis. Table 1 shows the list of drugs and general dosage levels used in treating Glioma tumor that develops in brain tissues [6].

Drugs used	Properties
Temozolomide	Molecular Formula: C6H6N6O2 Density:1.97gm/cm^3, Molecular Weight: 194.15
Avastin	Molecular Formula: C6638H1060N1720O2108S44 Density:1.03gm/cm^3 Molecular Weight: 149196.8162 g/mol
Lomustine	Molecular Formula: C9H16ClN3O2 Density: 1.35gm/cm^3 Molecular Weight: 233.6952 g/mol
Carmustine	Molecular Formula: C5H9Cl2N3O2 Density:1.46gm/cm^3 Molecular Weight: 214.05 g/mol

Table 1: Properties of anti-cancer drugs.

Blood-brain barrier

Some cells in the brain relate to tight joints between them and have some electrical resistance. These are called endothelial cells. These cells of brain form a barrier called blood-brain barrier which allows substances such as water, glucose and amino acids through diffusion while avoids entry of harmful toxins. Moreover, all the capillaries which are passing in the brain are connected and surrounded by the cells of brain tissue and forms a strong barrier to avoid invasion of infective substances and other toxins. In this scenario even the drugs given to target the tumors in brain are being obstructed by the blood-brain barrier. Many research studies have been made and many drugs are found and designed in the way to penetrate the brain's protective layer. However, when compared to tumors in other regions of human body, treating brain is more difficult due to the existence of the powerful protective mechanism. In this study the drugs Carmustine and Temozolomide, TNZ which are known for its ability of penetrating the blood-brain barrier was used.

Human equivalent dosage

Clinical trials on animals are done to evaluate the safe dosage for the extent of tumor spread in humans. The tumor cells of humans are placed and cultured in healthy animals such as mice and Guinea pigs and the drugs are administered to find the power of drugs in treating the tumor and the optimum dosage that can be given to kill the tumor. The obtained dosage after the successful trial was converted to the human dosage using human equivalent dosage. In this study, to convert the dosage, the following equation is used [6,12].

$$\text{H.E. D} = \boldsymbol{A.D} * ((\boldsymbol{A.W})/(\boldsymbol{H.W}))^{0.33} \text{ -----(1)}$$

Where H.E.D: Human Equivalent Dosage; A.W: Animal Weight in KG; H.W: Human Weight in KG; and A.D: Animal Dose in (mg/kg).

Flows in cerebral arteries

Flow velocity of blood in the arteries and veins mainly depends on the flow area and therefore the circulatory system of the human body, which consists of blood flow with different velocities at different regions. Both coronary and carotid arteries which are less in size experience lesser flow velocities. Parameters such as Reynolds number and Womersley numbers are used to calculate and analyse the velocities in every part of the body. For instance, less Reynolds value of 300 and Womersley parameter of 4 in the carotid arteries considered in this study explains the presence of very low velocities in those, when compared to other major arteries [13].

Modelling of blood fluid flow and drug distribution

In this, details of geometry design, physics of the flow model, use of species transport equations, and boundary conditions are explained.

Design of physical model for flow analysis

One of the main objectives of this study is to design a three-dimensional artery connected to capillary and the tumor region of brain, using the CT and MRI scan images of S tumor-affected patient. As it is difficult to model the geometry of capillaries with minute dimensions using general design software such as Creo, SolidWorks, expensive 3-D convertors and extensive design software are essentially needed for this task. However, software such as Mimics and 3D-Doctor are also being extensively used in designing realistic models for research purposes today. They offer equal level of flexibility in design of complex geometries. Currently most research is being conducted in modelling the biomedical field geometries as the simulation analysis pathways to innovation of many technologies [7]. At the same time even some design software's such as Space-Claim can also perform well in doing necessary modification in design when there is a point of integrating two different entities subjected to study. In this study, a realistic artery capillary system is designed using Space Claim software and is integrated with the tumor affected human brain. The human-brain is also modelled to the realistic dimensions using the MRI scans of the brain-tumor affected patients using the 3- D modelling software 3D-Doctor. However due to incomplete patients' data in the form of numerous MRI slices, the design modelling software gave up the partially modelled brain with cavity at the tumor. So, the partially modelled data is taken into the design software Space Claim and was reconstructed to the exact dimensions of complete brain with exact location of tumor using the raw data given by 3D-Doctor. Also, due to the incomplete data in design from the eight slices of scans considered in this study, some of the images at the ends of the brain were extracted from this to round out the incomplete brain obtained from the 3D-Doctor software. Using both the raw data's the design is developed in Space Claim software [17].

Design procedure and model description

The design and analysis algorithm for the computation flow and drug delivery is outlined in the figure 4.

Figure 4: Flow chart of design.

Initially the CT scan image of an adult is considered to model the above shown cerebral artery. The CT scan image shows several capillaries leading to various connections in the brain. However, for the simplicity of the design the partial part of the image is taken for modelling. As the part of design process, the image is inserted into the design window and splines are carried out with respect to the image curvature. Then the splines are connected to a completed 2-D planar image. The design software, Space-Claim used for this construction has the unique feature of prompting the three-dimensional plane to the complex curvature. Using the three-dimensional sweep options, the 3-D model is prepared as in figure 5.

Figure 5: CAD Design model constructed from CT scans.

Now the above-obtained model was designed by dividing the artery into three divisions and each capillary into a separate division. The extrude option is used in joining the pieces of 3-D parts created separately. These can be done in Space-Claim easily by dragging the images without using the assembly options. The above figure shows us the major cerebral artery of 14 mm diameter which flows into the brain with five capillaries leading to the tissues of the brain. The most complicated structures of capillaries, which are 2mm in diameter can be seen at each outlet divisions. Each capillary attached to the tissues is approximated to a certain length for making the design process simple. The connections at the major artery and capillary are done using the sweep extrude option of Space Claim which prompts insertion of the capillary to the major artery following the splines created as bounds for the extrusion. In this study the blood pumped by the heart to the cerebral arteries is considered as the inflow and the blood flows in the major artery followed by the smaller arteries and capillaries through the pump of heart called as systole phase.

Approximated tumor in tissue connection

The artery-capillary unit designed in the Space Claim design module is taken into the meshing software Hyper Mesh to do the mesh. Using the constructive options in Hyper Mesh a circular tissue and an elliptical tumor is designed and integrated to the available three-dimensional artery. figure 6 explains the design of CT scan.

Figure 6: 3D-Design from CT scan.

Reconstructed brain with tumor

To obtain the three-dimensional model of the realistic brain from the available 3-D modelling software, we need to have the slices of the patient's complete brain which are taken as MRI scans.

MRI scans typically in the form of number of slices, provides the accurate geometric features of the patient complete brain. Many slices of the brain in the form MRI scans are needed to convert the MRI-scans into a complete three-dimensional brain. The number of scans needed may vary from 80-120 depending on the accuracy of the model which has to be derived from the input scans. However, due to difficulty in finding the specific patient's personal data through the online resources, in this study, only eight slices of the MRI scans of a specific patient are considered in building up the three-dimensional model. The slices considered for this study consist of a tumor of volume 128.9 mm^3 at the distance of 13 mm and 7.3mm from the frontal part and the right side of the brain respectively. These slices are taken into the 3-D Doctor imaging software which prompts us to arrange the slices in the appropriate order of the human brain. It also allows us to copy the image repeatedly and arrange it an orderly manner. Now using the 8 slices the copies are made and arranged in an orderly manner to obtain the image with series of clicks. However due to the inadequate information in the form of slices the image obtained in the imaging software was a partial one. Then the obtained feature is modelled into the complete brain using space claim features such as loft, sweep etc. The final image obtained as the realistic brain is as shown in figure 7.

Figure 7: 3D-Design of reconstructed brain from MRI scans.

Now the previously designed artery is integrated into the tumor-affected brain cavity which was left apart during its design due to inadequate data at certain central portions of brain. The Space Claim software was again used for this job and the final unit of the brain with artery-capillary network is shown in figure 8.

Figure 8: Transparent and opaque 3D design views.

As an initial attempt, the velocity and pressure variations during the blood flow to the brain and tumor region are analyzed in the imaginary circular tissue region with an elliptical tumor. Then the model of realistic brain shown above is used for analyzing the blood supply and drug administration which reflects the real case scenario.

Selected physics for flow model

The real case scenario of modelling blood includes consideration of blood flow as two-phase flow as it contains red blood cells, White - Blood Cells and corpuscle suspend in serum, while blood behaves as a non-Newtonian fluid. However, due to the complexity in dealing with that real case flow of blood, the model in this study is initially simplified to Newtonian and then extended to non-Newtonian single-phase blood flow, which is further considered with drug inflow as another discrete phase.

Table 2 details are the physics assigned in modeling the blood and drug flow.

Newtonian and non- Newtonian fluid

Newtonian and non-Newtonian fluids are the fluids which obey and not obey the Newton's law respectively. As Newton's law says that shear stress is directly proportional to shear rate, Newtonian

Blood Flow	Newtonian with constant viscosity input, Implicit Unsteady, Constant density, Laminar, Segregated Flow	Non-Newtonian with varying viscosity input, Implicit Unsteady, Constant Density, Laminar, Segregated Flow
Drug Flow	N/A	Multi-phase, Eulerian - Lagrangian Model, Injectors, Spherical Particles, Liquid, Density, Particle Dimensions

Table 2: Physics assigned to the model.

fluids have the constant viscosity coefficient, whereas the other type of flow has varying viscosity coefficients as the shear stress and shear rates are not directly proportional to each other. Experiments on human blood vessels show the existence of Newtonian flow in large arteries [1]. However, smaller arteries and capillaries show non- Newtonian behaviour [8].

Viscosity of flow model

Several viscosity models are used for setting properties of the material for which the flow is calculated. However, in this study Carreau Yesuda model is used because of its known popularity in presenting the decreased velocity with applied shear strains, called shear thinning property. This model is suitable for non-Newtonian flow of blood in calculating the velocities at the wall [4,8].

$$\eta_{eff}(\gamma) = \eta_{\infty} + (\eta_0 - \eta_{\infty})(1 + (\lambda\gamma)^2)^{\frac{n-1}{2}} \quad (2)$$

Where η_0 = viscosity at zero shear rate, $\eta\infty$ = viscosity at infinite shear rate, =relaxation time, n = power index.

The values of 0.056 Pa-s, 0.004 Pa-s, 3.313 s, 0.3568 are used respectively for the above parameters.

Setting porous medium

The tissues of the brain are complex and exhibit porous nature. The nutrients carried by the blood will be delivered to the cells in the tissue in the form energy. The energy intake and waste disposals into the cells and venules are done by perfusion through the pores. In general, porous medium is defined as a group of closely bound particles, which exhibit a dispersible property in the liquid through which it flows [8]. Mathematically it is given as follows.

Total interface area

$$s = \frac{\text{Total Interface Area}}{\text{Total Volume}} \quad \text{---------(3a)}$$

$$\varepsilon = \frac{\text{Void Volume}}{\text{Total Volume}} \quad \text{---------(3b)}$$

Where S: Particular Surface

ε: Porosity.

Brinkman's flow model for porosity

Various models are utilized in analysing the porous nature of biological tissues. Darcy model is one of the basic models used in analysing flows in porous media. However, many other models such as Brinkman's and generalized Darcy models are derived by extending the Darcy model. These models are used in many experiments on analysis of mass transfer in porous medium and were tested for their suitability of usage in the regions of human body [2]. Results of experiments explain that Brinkman's porosity model could offer better results in analysing the mass transport in arteries near tissues. Since in this study, blood flow and drug distribution in two porous systems (i.e., tissue and tumor) are considered, Brinkman's model is used for defining porosity of the system.

Darcy and brinkman's models

According to Darcy flow model through a porous medium the drag force on the body is proportional to the viscosity of the fluid and velocity over the body, whereas Brinkman's model involves dealing with an extra term, comparable to the momentum diffusion term in the Navier-Stokes equation [12]. The following formula shows the mathematical representation of two models:

$$U = \left(\frac{G - \bar{\mu}\nabla^2 U}{\mu}\right) K \quad \text{---(4)}$$

Where U=Velocity of Blood, K= Porosity Parameter, μ= Viscosity of Blood and G= Pressure Gradient.

In this study, due to complexity in solving the Brinkman's model, the modified form, Brinkman's Forchheimer equation, which takes care of inertial and viscous terms, is considered. The viscous and inertial terms are calculated using the Ergun's empirical formula.

$$-\nabla P = \frac{\mu U}{K} + \beta \rho U^2 \quad (5)$$

Where $P_v = \frac{150\mu(1+-\aleph)^2}{\aleph 3 D 2}$ and $P_i = \frac{1.75\rho(1-\aleph)^1}{\aleph 3 D 1}$

Here the change the in pressure and variations of molecular viscosity in the above nonlinear equation are determined experimentally, whereas the porosity of the tissue and tumor regions is given as 0.3 and 0.2 as the white matter, i.e., tissue of brain has the porosity 0.3 [5].

Drug inflow model

Fluid flow can be represented mathematically in Eulerian and Lagrangian flow. The basic difference these two flows is the Eulerian flow model tracks particles with respect to a fixed origin considering the particle phase as a continuum. The equations in Eulerian are developed using conservation equations on a control volume basis, where as in Lagrangian type of flow the particles are considered as the dispersed phase and the particle tracking with respect to its path is done individually. Because of this quality, Lagrangian model is a good fit good. Our objective of this study is to trace the overall particle dispersion pattern. In this study the, Lagrangian flow model is considered based on the objective of the study [16]. The Lagrange equation for particle flow is given as:

$$(d\boldsymbol{U_p})/dT = F\,(U - \boldsymbol{U_p}) + G\,(\boldsymbol{\rho_p} - \rho)/\,\boldsymbol{\rho_p} + F1 \text{---} (6)$$

Where U_p: Particle velocity vector, F_1: Additional forces, F: Inverse of relaxation time and U: Fluid velocity.

The above equation is analogous to Navier-Stokes equation and shows the force balance of the particle flow. The first term in the right-hand side includes the drag force which is expected on the particle by the fluid. Here in this study, the relaxation time includes the terms drag force and coefficient of drag, which are derived from Stokes law as it works best for flows with minute cross-sections. The Reynolds number is calculated for this study considering the slip velocity of particle which is the relative velocity between fluid and particle. The obtained Reynolds number guides us to choose the drag models for the fluid study. In this study the obtained Reynolds number demands the use of Nauman-Schiller equation which is one of the drag models. The second term of the equation takes care of the gravity force exerted by the fluid flow on the particle. The additional forces in the form of viscosity changes due to porosity responsible for changes in the flow are also considered here. The below terms show the mathematical expressions considered in each term of the equation.

Coefficient of drag, $C_d = 24(1+0.15\,R_{EP}^{0.687})/R_{EP}$ -------(7)

Where

Reynolds number $R_{EP} = \rho v D/\mu$

$F = d^2\rho/(18\mu f_d)$ and $f_d = 0.5 c_d v_s^2 A\rho$

Designed simulation model

Healthy artery

The geometry of the healthy artery is as shown in figure 9 below. The length of the artery is 11mm and the diameter is 5mm. The capillary is of length and diameter 5 mm and 1.5 mm respectively. A tissue region assumed to be spherical with dimensions 320 mm^2 is also attached to the artery capillary-network. The geometry of the healthy artery-capillary system is as shown in the figure.

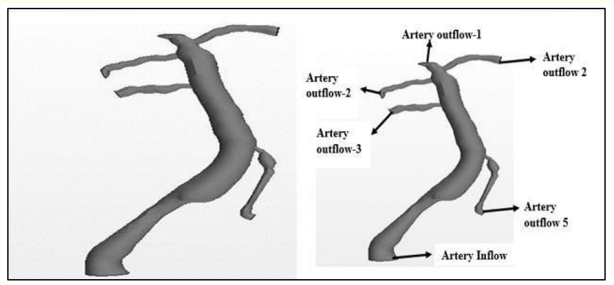

Figure 9: Geometry of the healthy artery capillary-network with healthy tissue.

Artery-capillary network with an imaginary tumor tissue

The geometry of the unhealthy imaginary tissue with Artery capillary network is as shown in the figure 10. A tumor in elliptical shape is present in the spherical tissue. The dimensions of the tumor are 120 mm^2.

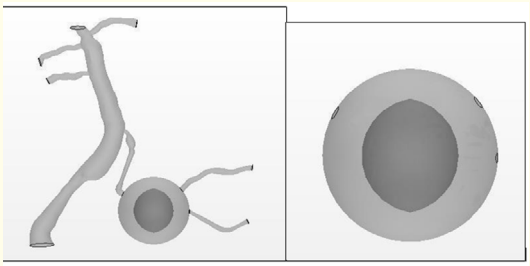

Figure 10: Geometry of the approximated tissue with tumor connected to artery-capillary network.

Model with reconstructed brain tissue

The geometry of the tumor-brain is as shown in figure 11. It has the average dimensions of 140 mm in length and 120 mm in width with the thickness of 110 mm. Also, the average dimensions of the tumor are 7.7 mm length, 4.65 mm width and 3.6 mm thick.

Figure 11: 3D model with tumor view.

Mesh generation for approximated healthy tissue with artery-capillary network

For this study Surface Remesher, Prism Layer Mesher and Trimmer are the mesh models used. The base size given is 0.03 mm with three number of prism layers and 25% thickness of the base size.

Unhealthy Tissue Artery-Capillary System:

Figure 12 shows mesh generation with number of cells for unhealthy approximated tissue artery-capillary system.

Mesh in an unhealthy spherical-shaped approximated tissue with tumor.

Artery mesh with node values.

Figure 12: Mesh distribution in tumor region.

Mesh generation for healthy and tumor-affected reconstructed brain tissue with artery- capillary network

The mesh of the realistic brain is generated using Hyper Mesh. The base value is given as 0.01 mm with three prism layers. The surface remeshing is done manually at the complex curvatures. The generated mesh for curved healthy and tumor-affected realistic brain tissue and artery system is shown in the figure 13.

Figure 13: Mesh of reconstructed brain tissue.

Governing equations

Navier-Stokes equation is used for analysing and computing the dynamics of flow. However, some assumptions are made in analysis depending on the requirement.

Blood flow

Initially analysis is done for finding the flow velocities and pressures in arteries carrying blood from heart to brain, both Newtonian and non-Newtonian natures of blood were analysed. For this the Navier-Stokes equation is considered as Newtonian incompressible and non-Newtonian incompressible respectively.

$$\rho\left(\frac{\partial u}{\partial t} + (u.\nabla)u\right) = -\nabla p + \mu.\nabla^2 u \quad \text{----- (8)}$$

The above equation is the general Navier-Stokes equation for incompressible flow.

This equation remains same for non-Newtonian flow analysis, but it must be modified for dealing with the other case. The modified equation is as shown below:

$$\rho\left(\frac{\partial u}{\partial t} + (u.\nabla)u\right) = -\nabla p + \nabla(\eta(\nabla u + (\nabla u)^T) \quad \text{-----(9)}$$

Here in the above equation the viscosity and shear rate vary with time.

Boundary conditions

Velocity inlet with transient velocity data input

The set of tabulated values is given as input velocity table for inlet of artery. This velocity data is observed from the waveform calculated by Hashimoto [17] as demonstrated in figure 1 in section 2.1. The changes of velocities with respect to time is shown in table 3.

Variable	Velocity range (cm/sec)
Systolic forward peak velocity (V_F)	69 ± 19
Diastolic reverse peak velocity (V_R)	-19 ± 6
End diastolic velocity (V_D)	8 ± 4
Time-averaged mean velocity (V_M)	1 ± 3

Table 3: Velocity Range with Respect to Varying Velocities.

Input for drug flow model in multiphase lagrangian flow

To set the particle flow for analysing the drug concentration distribution, Lagrangian multiphase flow is considered. A separate physics is set for analysing particle flow in the artery- capillary-tissue-tumor network. The flow rate is given an inlet to the artery using Lagrangian injectors. Also, particle specifications such as diameters and shape are specified. The table 4 shows the flow input and particle specifications given to analyse the flow.

Concentration	Particle Diameter	Particle density
0.01 mL	5.0 MICRON	1460 Kg/M^3
0.03 mL 0.05 mL 0.08 mL	0.5 MICRON	1960 Kg/M^3

Table 4: Drug Particle Parameters.

Unsteady computational parameters

Simulations are carried out considering the segregated flow solver to solve the flow equations. The solution update in star CCM+ for the segregated model is done using the SIMPLE solver. In this study, the first-order discretization is used to solve this problem and results are drawn at different time steps with the maximum physical time of 0.8sec, time step of 0.01sec and 50 inner iterations for each time step. Also, under-relaxation factors of 0.7 and 0.3 are considered for velocity and pressure respectively.

Results and Discussions

The computational simulation model developed is used to determine the velocity and pressure changes in the flow of blood with respect to the cardiac cycle in the brain region with porous tissues. Further particle distribution of drug administered into the targeted tumor region is observed in terms of velocities with which drug reaches the target. Also, the various of concentrations administered are analysed for particle velocity with changed particle size, density, concentration distributions and optimized the concentration to determine as the maximum safest drug dosage to treat tumor in brain.

Blood flow in the artery with approximated tissue-tumor region

Pressure variations

Figure 14 show the variation of pressure distribution for both healthy and tumor regions of brains tissue connected to the ar-

tery-capillary network. Selected time is 0.01s, 0.1s and 0.25s. A significant variation in the pressure with time is noticed between the healthy and tumor region of the brain-tissue connected to the artery-capillary network. For example, in, in figure 14 (a) at time 0.01s, pressure ranging from -701.9 pa to 2583.3 pa for the healthy case, whereas the pressure level is reduced significantly to a range of -49.9 pa to 641.72 pa for the tumor case. Similar trends are also notice with increase time to 0.1s and 0.25s. In specific, the tissue region of brain faces the pressure ranging from -44.86 pa to 612.18 pa in a healthy artery where increase in pressure range is observed in tissue region due to the presence of tumor.

Figure 14: Pressure variation at time Pressure at 0.1 Sec.

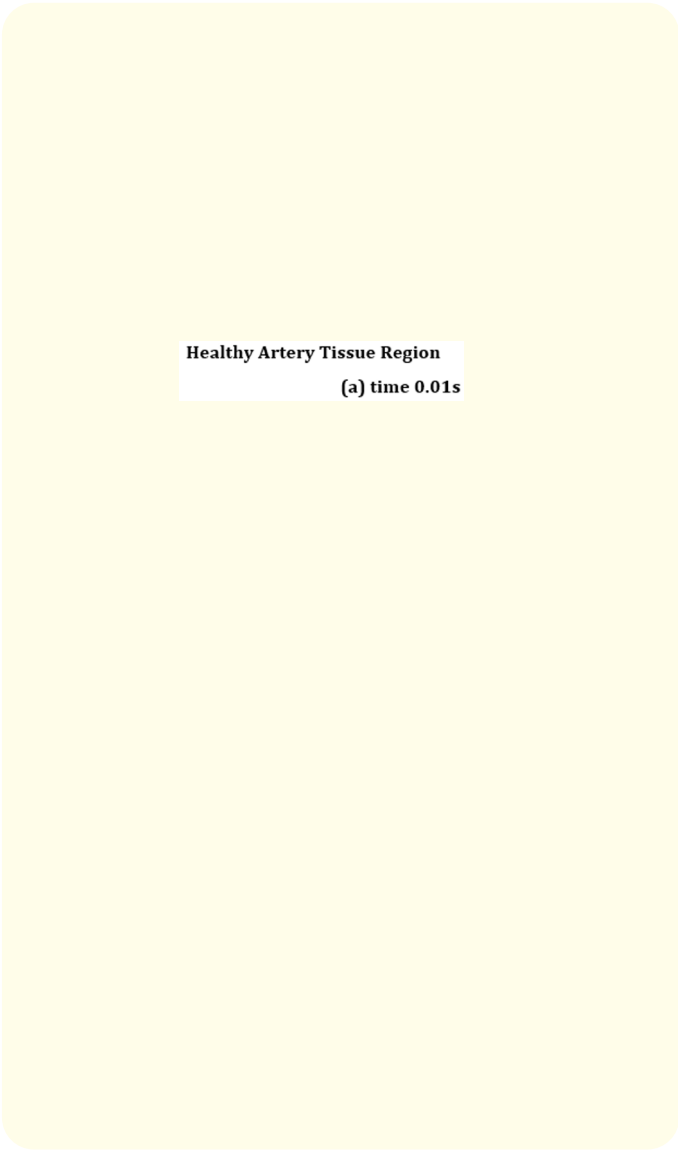

Figures 14 (b) show the pressure distribution varying from -985.90pa to 3180.3 pa for healthy artery-tissue and -1125pa to 3605 pa. tumor artery-tissue region respectively. Here the tumor tissue region of brain faces the pressure ranging from -179 pa to 767pa in which there is an increase in pressure of 24% from the previous reading shown for time 0.01s. In figure 14(c) at time 0.24s the pressure ranges from -905pa to 3620 pa for healthy arterytissue and it ranges from -1243pa to 3666 pa in the tumor artery-tissue region. Here the tumor tissue region of brain faces the pressure ranging from -500 pa to 726pa, which is comparatively 34% less than from the pressures at 0.1 sec.

Velocity variations

Figures 15(a) and 155(b) shows the velocity distribution of healthy and tumor regions of brains tissue connected to the artery-capillary network. The velocity ranges from 0 to 3.98m/sec in non-tumor case and 3.78m/sec in tumor case, with less velocity in regions of tumor and tissue. The figure more precisely shows the values in closer range, which is fixed to max scale of 0.05m/sec to show the velocity in tumor region. The above figures show the obstruction created by the tumor for the blood flow thereby reducing the velocity in the tumor tissue region.

Figure 15: Velocity distribution at time.

The figure 16 shows the velocity distributions at the 0.1s-time step with respect to position. The x-axis is taken as the diameter of the artery tube and the y-axis shows the velocity values. The non-Newtonian velocity of tumor and healthy velocity lies in between the values of Newtonian velocity range. Newtonian model generally cannot predict the accurate values at the regions such as large and minor arteries [18].

Figure 16: Velocity plots which shows comparisons of velocities with respect to diameter.

Figure 17(b) shows the velocity variation with respect to position of the artery. As we move from left to right with respect to position on x-axis as shown in figure 17 a(a), the velocity decreases around capillary due to higher resistance. The values vary from 1.4 m/sec in higher arteries to 0.18 and 0.15 at lower arteries. This shows the real mechanism of blood flow from heart to capillaries, which is generally lower to allow time for exchange of species and energy to tissues. Since the values are higher for major arteries, the plots shown above include two set of values that show both the flows in major arteries, which are much higher than that in regions other than capillaries. In the above plot, the lines obtained with the artery-velocity is represented by the line with left sided arrow whereas the rest of the flow lines are shown with right arrow.

The plot in figure 17(c) shows the pressure distribution at 0.1, 0.25, 0.5 time. The pressure reduces with the resistance to flow due to obstruction and so there is a pressure variation in the tissue tumor region. The artery at 2 mm shows the highest pressure as there is no obstruction to the flow, whereas the capillaries and tumor-tissue region have lower pressure. Then the outflows are shown with raised pressure due to the suction created at the heart valves demanding the next cardiac cycle to start and repeat. The plot here is also considering the points shown in figure 4.8 as the points of interest to observe changes in pressures. However due to huge changes in values between the artery and the other areas, even here the secondary axis is taken to show the changes in the above plot. Here the dotted line with a left arrow marking shows the pressure changes with time in the major artery and the values, shown at the side of left-handed arrow, represent the respective values of major artery at different times, whereas the right-hand side values are the values of the rest of the regions at different time.

(a) Selected Points considered to draw plots with respect to position from the reference

(b) Velocity plots with respect to position

(c) Pressure Variations with respect to position

Figure 17: Blood flow with respect to position.

Results for drug distribution in the artery with tissue-tumor Connection

For the initial case analysis, the drug Temozolomide is used with concentrations in safe range of 0.03 mL -0.08 mL using the advection diffusion principle in multiphase Lagrangian modelling. In this initial case study, particle velocities of drug with concentrations of 0.03 mL, 0.05mL, and 0.08 mL are observed with changed particle dimensions values of 5, 0.5 Microns. The below results are obtained at times from 0.1-0.5s of cardiac cycle for the changed concentrations and changed particle dimensions.

Drug particle velocity and concentrations with 0.03 ml concentration

The figure 18(a) shows the particle velocity at 0.1s when a dosage of 0.03mL is inserted into the blood stream. The highest velocity with which the particle flows is 4m/sec. However, the tissue and the tumor regions receive blood flow with lesser velocities which is numerically not very clearly visible in this figure.

(c) 0.2s (d) 0.25s

(e) 0.3s (f) 0.4s

Figure 18: Particle velocity with 0.03mL.

The figure 18(b) shows the particle velocity at 0.125s when a dosage of 0.03mL is inserted into the blood stream. The highest velocity with which the particle flows is 4.7m/sec.

However, the tissue and the tumor regions receive blood flow with lesser velocities which is numerically not very clearly visible in this figure. Also, it is the highest velocity observed with in the cardiac cycle. We can also observe increased particle flow due to the increased cardiac input into the tumor tissue region compared to previous and the other flows at various time shown.

The figure 18(c) shows the particle velocity at 0.2s when a dosage of 0.03mL is inserted into the blood stream. Here the particle flows with a maximum velocity of 3.5m/sec. We can also observe a downfall of particle flow due to the change in cardiac input into the tumor tissue region compared to previous flow. However, the particle concentration in the tumor tissue region appears almost like the case of 0.125s. The figure 18(d) shows the particle velocity at 0.25s with the particle flows with a maximum velocity of 3.4m/sec. We can observe at this stage majority of particle flow is very slow in velocity in both artery and tumor region compared to previous flow. However, the particle concentration in the tumor tissue region appears almost like the case of 0.125 and 0.2 time.

The figure 18(e) shows the particle velocity at 0.3s reaches a maximum particle flow velocity even drops to 2.2m/sec resembling the cardiac cycle. We can also observe less flow in the arterial region compared to the tumor tissue regions are the half cycle is completed at this stage. The figure 18(f) shows the particle velocity 0.79m/sec at 0.4s. Also, only few particles are observed in the artery regions as the cycle is being finished.

Drug particle velocity and concentrations with 0.05 ml dosage

Figure 19 show variation drug particle velocity with time following a cardiac cycle and for a drug dose of 0.05ml.

(a) 0.1s

(b) 0.125s

(c) 0.2s

(d) 0.25sec

(e) 0.3s

(f) 0.4s

Figure 19: Particle velocity with 0.05mL dosage at different times at 0.1sec.

Figure 19(a) shows the particle velocity at 0.1 time when a dosage of 0.05m is inserted into the blood stream. The value obtained at this time step is 3.987 m/sec, which is the maximum value observed at the arterial flow. However, the tissue and tumor regions are shown with semi-filled particle flow with lower velocities ranging from 0 to 0.7973 m/sec.

Also, only a few particles are observed in the artery regions as the cycle is being initiated. figure 4.19(b) shows the particle velocity at 0.125s when a dosage of 0.05 ML is inserted. The highest velocity is obtained at this time step and the observed velocity is 5.6852 m/sec. However, the tissue and tumor regions are shown with filled particle flow with lower velocities ranging from 0 to 1.1370 m/sec. Also, increased concentration of particle flow is observed at this time step. figure 4.19(c) shows the particle velocity at 0.2s. The highest velocity is obtained at this time step and the observed velocity is 4.41 m/sec. However, the tissue and tumor regions are shown with filled particle flow with lower velocities ranging from 0 to 0.8825 m/sec. Also, increased concentration of particle inflow is observed at this time. The figure 19(d) shows the particle velocity at time 0.25s. The highest observed velocity currently is 2.8840 m/sec. However, the tissue and tumor regions are shown with filled particle flow with similar concentrations to the previous time. figure 19(e) shows the particle velocity at time step 0.3s. The highest observed velocity currently is 1.85 m/sec. While the tissue and tumor regions are shown with filled particle flow, the arteries show less particle flow. figure 19(f) shows the particle velocity at time step 0.4s. The highest observed velocity currently is 0.33846 m/sec. Here the tissue and tumor regions are shown with filled particle flow with similar concentrations to the previous time, but there is very much less particle flow in arterial region.

Comparison of velocities with respect to concentration in increasing order: 0.1 time

Figure 20 shows the particle velocity change at time step 0.1s with a change in dosage from 0.03 mL to 0.08mL. The highest observed velocity currently is 3.9 m/sec for 0.03 mL and least for 0.08 mL as 3.5 m/sec. Then the velocity decreased with increase in concentration.

Figure 20: Changes in particle velocity changes at tissue-tumor region at 0.1s.

Figure 20 shows the particle velocity change at time step 0.1s with a change in dosage from 0.03mL to 0.08mL. The highest observed velocity currently is 3.9 m/sec for 0.03 mL and least for 0.08mLas 3.5 m/sec. Then the velocity decreased with increase in concentration.

Figure 21 shows the particle velocity change at time 0.125s with a change in dosage from 0.03 mL to 0.08 mL. The highest observed velocity currently is 4.7 m/sec for 0.03mL. Then the velocity decreased with increase in concentration.

(c) 0.08mL

Figure 21: Particle velocity changes at tissue-tumor region at 0.125s.

Figures 22 shows the particle velocity change at time step 0.3 time with a change in dosage from 0.03 mL to 0.08mL. The highest observed velocity currently is 1.9 m/sec for 0.03 mL and least for 0.08 mL as 1.09 m/sec. Then the velocity decreased with increase in concentration.

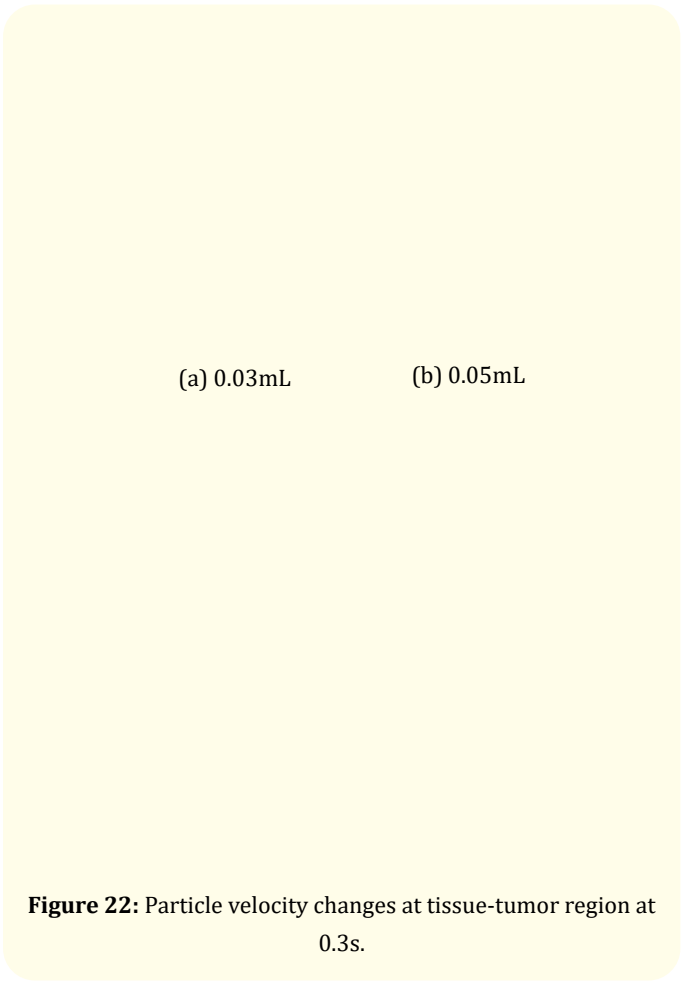

(a) 0.03mL (b) 0.05mL

Figure 22: Particle velocity changes at tissue-tumor region at 0.3s.

Figures 23 shows the particle velocity change at time step 0.4s with a change in dosage from 0.03 mL to 0.08mL. The highest observed velocity currently step is 0.79 m/sec for 0.03 mL and least for 0.08mLas 0.047m/sec. Then the velocity decreased drastically with increase in concentration and due to the decreased blood flow through cardiac input.

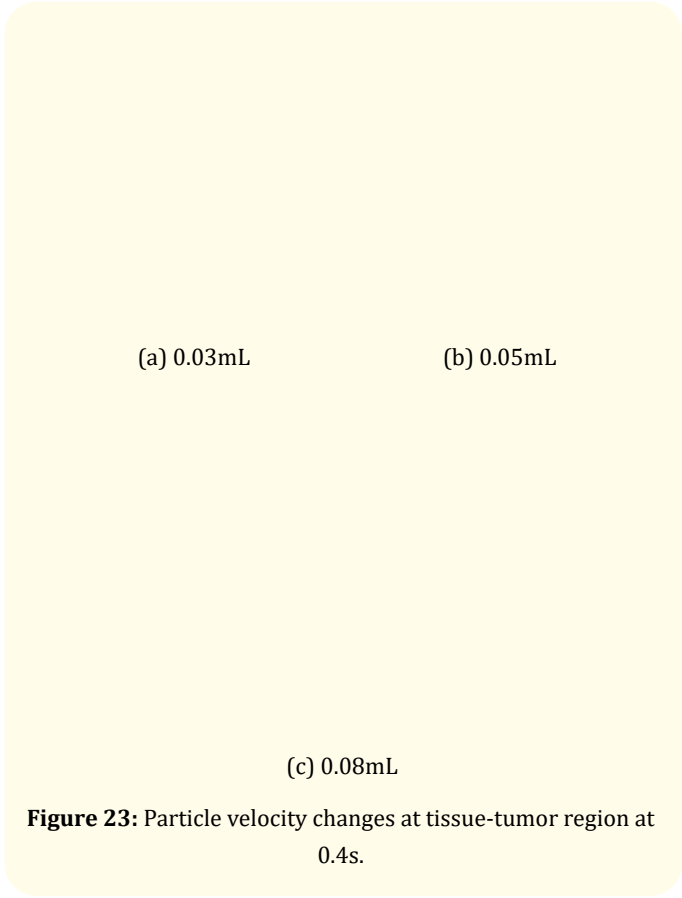

(a) 0.03mL (b) 0.05mL

(c) 0.08mL

Figure 23: Particle velocity changes at tissue-tumor region at 0.4s.

To analyse the velocity in the vicinity of tumor, a line probe originating from the capillary and passing through the tumor is drawn. The following results show the velocity changes in the tumor at the central area.

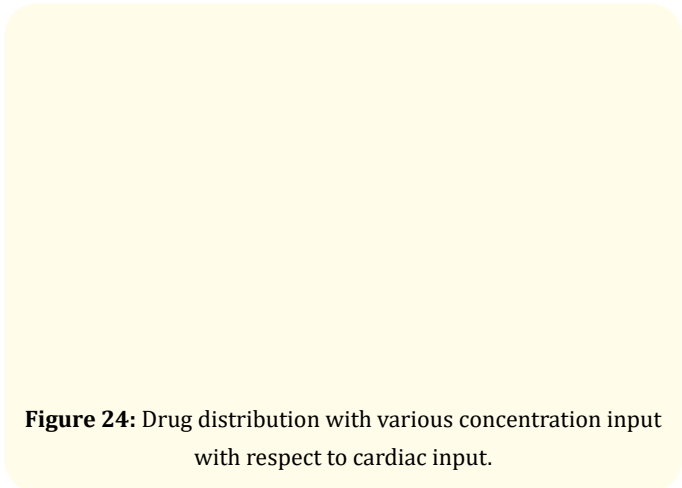

Figure 24: Drug distribution with various concentration input with respect to cardiac input.

The plot in figure 24 shows the velocity with which the particle penetrates the tissue tumor region with different input concentrations. It is observed that with increase in concentration the particles are moving with slower velocity into the regions of tissue and tumor. However, each input is following the cardiac input cycle. This plot can only emphasize the effect on velocity with increase in concentration. But to show the particles which are entering into the tissue region we must see the particle count or volume fraction.

Concentration at line probe

Velocity alone cannot assure us to find out the effect of drug in the site of tumor. Concentration distribution analysis gives better idea. figure 25(a) shows a line probe passing through the tumor is drawn to analyze the concentration of drug particles at that site. figure 25(b) shows the distribution variation with respect to drug changes. It is observed in plot that with increase in dosage there is huge increment in particle settling at the target region. But there is less difference observed with the concentration increase from 0.05 mL to 0.08 mL.

(a) Line Probe

(b) Concentration at line probe with varying dosage levels

Figure 25

Results for drug distribution in reconstructed brain

For this case two drugs which can cross the protective barriers of brain are considered. The densities of the drugs are 1460 kg/m^3 and 1960 kg/m^3 respectively. Using the human equivalent drug dosage estimation, the dosages of 0.01 mL, 0.03 mL and 0.0 5mL are considered as administering dosages for this study. The following results are obtained at time steps from 0.1-0.5 sec of cardiac cycle for the changed concentrations,

Drug particle velocity and concentration with 0.01 ml concentration

Figure 26(a) shows the particle velocity at 0.1s when a dosage of 0.01mL is inserted into the blood stream. The highest velocity with which the particle flows is 3.8203m/sec. However, the tissue and the tumor regions receive blood flow with lesser velocities which are numerically negative. figure 26(b) shows the particle velocity at 0.125 time when a dosage of 0.01 mL is inserted into the blood stream. The highest velocity with which the particle flows is 4.5230 m/sec. However, the tissue and the tumor regions receive blood flow with lesser velocities. There is an increased particle flow due to the increased cardiac input into the tumor tissue region compared to previous and the other flows at various times shown. 26(c) shows the scaled particle velocity at 0.25 time when a dosage of 0.01 mL is inserted into the blood stream. Here the maximum particle velocity observed is 1.8m/sec. figure 26(e) shows the particle velocity at 0.5 time when a dosage of 0.01 mL is inserted into the blood stream. The values obtained at this time is 1.17m/sec. Here only few particles are observed in the tissue regions and concentrated particle at the tumor region as the cycle is being finished.

(a) 0.01s (b) 0.125s

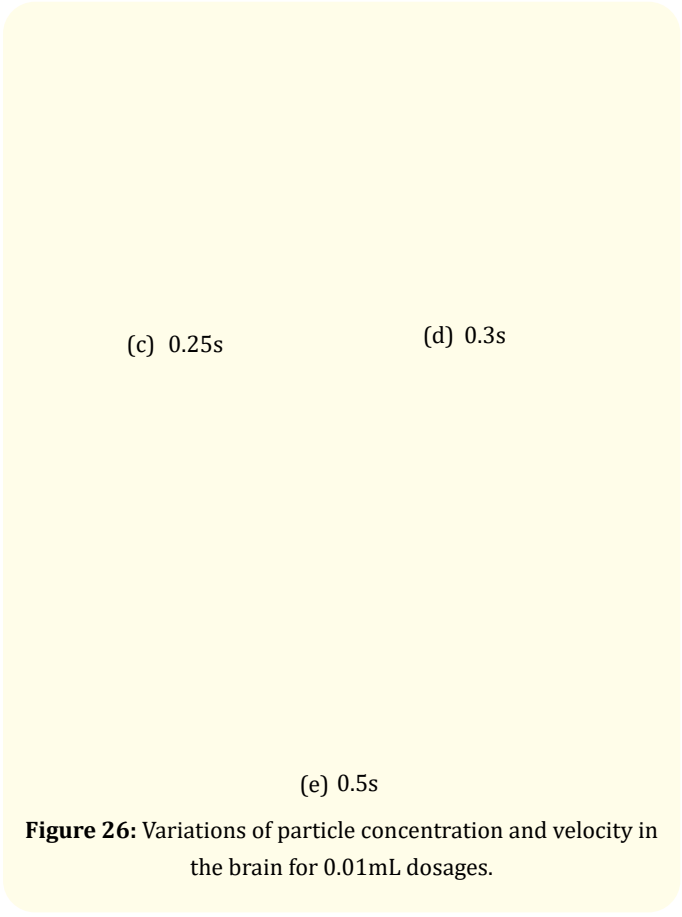

(c) 0.25s (d) 0.3s

(e) 0.5s

Figure 26: Variations of particle concentration and velocity in the brain for 0.01mL dosages.

Drug particle velocity and concentration with 0.03 ml dosage

Figure displays variation of drug concentration and velocity strength for a dosage of 0.03 mL.

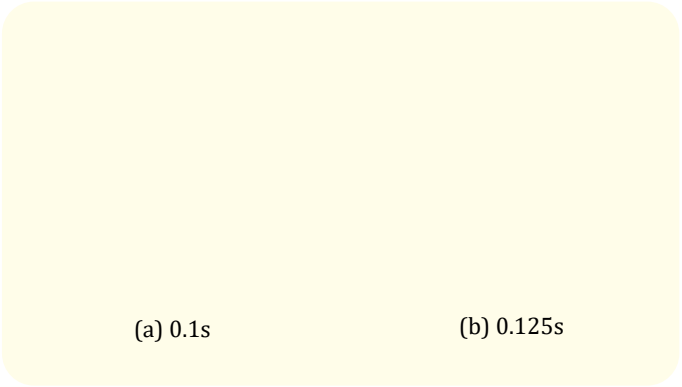

(a) 0.1s (b) 0.125s

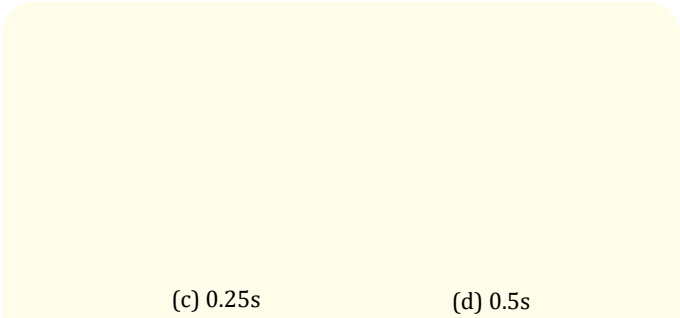

(c) 0.25s (d) 0.5s

Figure 27: Particle velocity in reconstructed brain at 0.1 time with 0.03mL.

Figure 27(a) shows the particle velocity at 0.1 time when the drug dosage of 0.03 mL is inserted into the blood stream. The highest velocity with which the particle flows is 3.8425m/sec. The tissue and the tumor regions receive blood flow with lower velocities compared to the 0.01 mL dosage. But, in both cases, values are numerically negative. figure 27(b) shows the particle velocity at 0.125 time when a dosage of 0.03 mL is inserted into the blood stream. The highest velocity with which the particle flows is 4.48 m/sec. This velocity is the highest peak velocity observed during the cardiac cycle at this time step reflecting the highest drug flow. Even here the tissue and the tumor regions receive blood flow with lesser velocities of 1.405E-9 m/sec. figure 27(c) shows the particle velocity at 0.25 time when negative cycle part. Here the particle flows with a maximum velocity of only 1.1021 m/sec. The scale of d magnitudes shows the better view of changes in particle velocity. In this time the particle velocity is least, and it reaches the value of 2.887E9 m/sec, which is the least velocity observed through the cycle. figure 27(d) shows the scaled particle velocity at 0.5 time when a dosage of 0.03 mL is inserted into the blood stream. The highest velocity values obtained at this time is 1.08 m/sec at the artery and 4.0065E-8 at the target area. Here an only few particles are observed in the tissue regions and concentrated particle at the tumor region as the cycle is being finished. However, the particle velocity raised with respect to rise in cardiac cycle flow.

Drug particle velocity and concentration with 0.05 ml dosage

Figure 28 displays variation of drug concentration and velocity strength for a drug dosage of 0.05 mL. figure 28(a) shows the particle velocity variation at 0.1 time when the drug dosage of 0.05 mL is inserted into the blood stream. The highest velocity with which

the particle flows is 3.9 m/sec. However, the tissue and the tumor regions receive blood flow with lower velocities compared to the 0.01 mL dosage.

(a) 0.1s (b) 0.125s

(c) 0.25s

(d) 0.5s

Figure 28: Figure displays variation of drug concentration and velocity strength for a drug dosage of 0.05 mL

The Figure 28(b) shows the particle velocity at 0.125s when a dosage of 0.05 mL is inserted into the bloodstream. The highest velocity of the particle flows is 4.5004m/sec. This velocity is the highest peak velocity observed during the cardiac cycle at this time step, reflecting the highest drug flow. Even here the tissue and the tumor regions receive blood flow with lesser velocities of 5.56E-10m/sec. figure 28(c) shows the scaled particle velocity at 0.25 time when a dosage of 0.05 mL is inserted into the blood stream. The values obtained at this time step is 1.0021m/sec at the artery and 4.46E-10 at the target area which is the least velocity observed through the cycle. Here only few particles are observed in the tissue regions and concentrated particle at the tumor region. figure 28(d) shows the particle velocity as 0.05 time. Here the particle flows with a maximum velocity of only 4.5230 m/sec can be observed. The scaled magnitudes show the clear view of changes in particle velocity. At this time, the particle velocity is least, and it reaches the value of 1.9E8m/sec, due to rise observed at the point of the cycle.

Figure 29 shows the rate of penetration of the drug with different concentrations in the tumor region of the brain.

Figure 29: Rate of penetrations of the drugs with different concentrations in the tumor region of the brain.

Figure 29 shows the velocity penetrations of the drug with different concentrations in the realistic brain at the site of tumor. A line plot passing through the tumor from the input as artery is considered to see the results. As shown in the plot for the three different dosage inputs the velocity of 0.01 mL is far highest when compared to the other two dosages. If the values are scaled on per-

centage, the 0.01 mL velocities are 10% higher at the peak velocity of cardiac cycle and 5% ~~of the~~ cycle at the negative phase of cardiac cycle and then the percentage reduced to 2%. But the other two drug dosages gave almost nearer penetration velocity at every time step with less reach of drug to out of target areas. Also, the results of drug flow show much delivery of drug at 0.03 mL when compared to 0.05 mL where the particles also carried away to other parts in more quantity compared to 0.03 mL case. With this, we can say that 0.03 mL could be the optimal drug dosage for this case as there is no big change observed in the penetration velocity for the two dosages. However, only velocity penetration could not definitely act as the deciding factor. Therefore, concentration of particles at the site of tumor is to be analysed.

Drug concentration distribution in brain and tumor site

The concentrations at times 0.25s and 0.5s are observed to analyse the concentration at the target region for different dosages: 0.01 mL, 0.03 mL and 0.05 mL. Since the two types of flows considered here are liquids concentrations are shows as the volume fractions. Also, the results are scaled and magnified such that the highest volume that can be sown in the figure is 55000 as it clearly shows the fate of concentrations of particles that the tumor area.

Figure 30: Variation in drug concentration in tumor site with different input dosages.

We can observe that with the increase in dosage the concentration at the tumor site and the healthy regions are increasing. However, we can see the lowest concentrations at the site of healthy regions in each case. But if tumor targeting is considered which is the main objective of this study keeping in mind that healthy tissue should not be targeted more, 0.03 mL dosage does the good job in delivering the target with adequate dosage. Even though the highest dosage 0.05 mL is showing high concentrations than the 0.03 mL, it also shows highest concentration of 1.478 at the non-tumor region which is 50% more than the value 0.5057 shown at non-tumor sites for 0.03 mL distribution. Also, the difference observed in the concentration changes at the tumor site for both the concentration 0.03 mL and 0.05 mL are very small in numerical value which prompts us to choose 0.03 mL as the safe value that can be administered to treat the target area.

To find the optimal dosage other than the concentration distribution details, we also need to know the effect of particle size and particle type of the drug. For that study a line probe is drawn at the site of tumor crossing from artery to tumor from left to right and the effects of penetration velocity changes are observed on plots by changing the parameters. The plots shown in figure 31 explains the differences in penetration velocity with respect to size and particle type.

Figure 31: Penetration velocity with change in diameter.

The plot in figure 31 shows the velocity of drug *Carmustine*, which has the density 1460 kg/m^3 at different time steps with change in particle diameter. Two particle diameters are analysed for the penetration velocity and the plot shows that the lowest particle size of the drug penetrates with more velocity when compared to highest diameter size. This shows that the lowest diameter 0.5 microns can get into the pores of the tumor effectively when compared to the other size 5 microns.

This plot in figure 32 shows the penetration velocity with change in particle type. Two drugs Temozolomide and Carmustine, which are commonly used as anti-cancer drugs are used here. The

plot shows the velocity penetrations with change in density considering the effects of gravity. It is seen that the lowest density drug can penetrate better into the target region when compared to high-density drug. However, to justify the diameter of the particle must be considered.

Figure 32: Penetration velocity with change in density.

Figure 33 shows the plot which shows variation with density of the drugs with two different diameters.

Figure 33: Penetration velocity with change in particle size and type.

Results show that for change in diameter, two different drugs have shown increase in velocity with a decrease in diameter. However, if density is considered, the low-density drug with lower diameter is seen to be more penetrating effect than the higher-density drug.

Finally, the concentrations are plotted with respect to changed particle type at the site of tumor. figure 34 show Concentration variation with change in particle size and type. From the plot, we can observe that the concentrations are higher for the higher-density drug only at the highest peak velocity, whereas the rest of the plot shows almost equal concentrations, which prompts the result that low density drug can surround the target more when compared to high.

Figure 34: Concentration variation with change in particle size and type.

Conclusion

A computational simulation model has been developed for analysing the blood flow and drug concentration distribution in cerebral regions including the artery capillary network. The computational analysis is done by solving governing equations of blood flow dynamics based on Navier-Stokes equations and mass species transport based on Lagrangian particle flow equations. The diffusion considered in the capillary-tissue regions is based on brinkman's model. Analysis of blood flow is performed using experimentally derived cardiac input as inflow and considering the blood as non-Newtonian in nature which is closer to reality. The drug concentration distribution is also observed around the tumor, which is originated in the cerebral regions, assigning it with anisotropic porosity. The drug distribution is done through intra-venal administration with the administered drug parameters varying as

0.03 mL to 0.05 mL in dosage, 1460 kg/m^3 and 1960 kg/m^3 and 0.5 to 0.05 microns in particle size. The simulation analysis results shows that the increase in dosage has little effect on the target after a certain amount of dosage. It also explains us that the decrement in particle diameter and density as a combination could prompt us with better penetration effect of the drug to the tumor.

Bibliography

1. Jhunjhunwala P., *et al.* "CFD Analysis of Pulsatile Flow and Non-Newtonian Behaviour of Blood in Arteries". *Molecular and Cellular Biomechanics* 12.1 (2015): 3747.

2. Khaled A and Vafai B. "The Role of Porous Media in Modelling Flow and Heat Transfer in Biological Tissues". *Heat and Mass Transfer* 46.26 (2003): 4989-500.

3. Yamaguchi T., *et al.* "Computational Blood Flow Analysis-New Trends and Methods". *Journal of Biomechanical Science and Engineering* 1.1 (2006) 29-50.

4. Yilmaz F and Gundogdu MY. "A Critical Review on Blood Flow in Large Arteries; Relevance to Blood Rheology, Viscosity Models, and Physiologic Conditions". *Korea-Australia Rheology Journal* 20.4 (2018): 197-211.

5. Arifin DY., *et al.* "Chemotherapeutic Drug Transport to Brain Tumor". *Journal of Controlled Release,* 137.3 (2009): 203-210.

6. Bello L and Carroll RS. "Low-dose Chemotherapy Combined with an Antiangiogenic Drug Reduces Human Glioma Growth in Vivo". *Cancer Research* 61.20 (2001): 7501-7150.

7. Shafiullah M and P Majumdar. "Computational Fluid Dynamics Analysis of Blood Flow through Stented Arteries". Proceedings of the ASME 2013 International Mechanical Engineering Congress and Exposition (2013).

8. Narmada S. "CFD Analysis of Blood Flow through Stenosed Arteries". M.S. Thesis, Northern Illinois University, DeKalb, IL (2014).

9. http://www.nhlbi.nih.gov/health/health-topics.

10. "Brain Tumor Treatment Options".

11. Djamil F. "Brain Imaging in Arystoma".

12. "Properties of Chemo Drug used for Brain Tumor" (2015).

13. Womersley JR. "Method for the Calculation of Velocity, Rate of Flow and Viscous Drag in Arteries when the Pressure Gradient is known". *The Journal of Physiology* 127 (1995): 553-563.

14. Resmi SA and Thomas T. "A Semi-automatic Method for Segmentation and 3D modeling of Glioma Tumors from Brain MRI". *Journal of Biomedical Science and Engineering* 5.7 (2012): 1-6.

15. "Solid Works image" (2009).

16. Zhang Z and Chen Q. "Comparison of the Eulerian and Lagrangian Methods for Predicting Particle Transport in Enclosed Species". M.S. Thesis, Purdue University, West Lafayette, IN (2012).

17. Hashimoto J and Ito S. "Pulse Pressure Amplification Arterial Stiffness and Peripheral Wave Reflection Determination Pulsatile Flow Waveform of the Femoral Artery". *Hypertension* 56.5 (2010): 926-933.

18. Siebert MW and Fodor PS. "Newtonian and Non-Newtonian Blood Flow Over a Backward Facing Step-A Case Study". Proceedings of the COMSOL Conference (2009): 1-5.

Volume 2 Issue 12 December 2021